

Activation of Vav by the Gammaherpesvirus M2 Protein Contributes to the Establishment of Viral Latency in B Lymphocytes

Lénia Rodrigues,^{1,2} Marta Pires de Miranda,^{1,2} María J. Caloca,³ Xosé R. Bustelo,^{3*} and J. Pedro Simas^{1,2*}

Instituto Gulbenkian de Ciência, Rua da Quinta Grande 6, 2780-156 Oeiras, Portugal¹; Instituto de Microbiologia e Instituto de Medicina Molecular, Faculdade de Medicina, Universidade de Lisboa, 1649-028 Lisboa, Portugal²; and Centro de Investigación del Cáncer, Instituto de Biología Molecular y Celular del Cáncer (IBMCC) and Red Temática Cooperativa de Centros de Cáncer, CSIC-University of Salamanca, Campus Unamuno, E-37007 Salamanca, Spain³

Received 20 December 2005/Accepted 5 April 2006

Gammaherpesviruses subvert eukaryotic signaling pathways to favor latent infections in their cellular reservoirs. To this end, they express proteins that regulate or replace functionally specific signaling proteins of eukaryotic cells. Here we describe a new type of such viral-host interaction that is established through M2, a protein encoded by murine gammaherpesvirus 68. M2 associates with Vav proteins, a family of phosphorylation-dependent Rho/Rac exchange factors that play critical roles in lymphocyte signaling. M2 expression leads to Vav1 hyperphosphorylation and to the subsequent stimulation of its exchange activity towards Rac1, a process mediated by the formation of a trimolecular complex with Src kinases. This heteromolecular complex is coordinated by proline-rich and Src family-dependent phosphorylated regions of M2. Infection of Vav-deficient mice with gammaherpesvirus 68 results in increased long-term levels of latency in germinal center B lymphocytes, corroborating the importance of the M2/Vav cross talk in the process of viral latency. These results reveal a novel strategy used by the murine gammaherpesvirus family to subvert the lymphocyte signaling machinery to its own benefit.

The persistence of herpesvirus in the infected organism is dictated by the establishment of latency in particular cell types within the host. In the case of gammaherpesviruses, such as the human pathogens Epstein-Barr virus (EBV) and Kaposi's sarcoma-associated herpesvirus (KSHV), latency occurs by maintenance of the viral genome in the nuclei of infected B lymphocytes. To favor such a process, these viruses have developed a number of strategies aimed at interfering with different aspects of the host cell signaling machinery. For instance, the EBV genome encodes two proteins, latent membrane protein 1 (LMP1) and LMP2, which contribute to the activation of naïve B cells by mimicking the function of two important B-cell surface receptors, the CD40 molecule and the B-cell receptor, respectively (9). The spurious activation of the downstream pathways of those receptors by LMP1 and LMP2 contributes to B-cell activation, differentiation, and the rescue of infected germinal center (GC) B-cell blasts into the memory B-cell pool (36). Similarly, the K1 and K15 proteins encoded by KSHV can alter B-cell signaling by promoting the activation of the NF- κ B and the nuclear factor of activated T cells. In addition, they interfere with the function of tyrosine kinases and tumor necrosis factor receptor-associated factors (9). It is likely that the viral machinery devoted to the manipulation of the signaling pathways of host cells is not restricted to these

examples. Indeed, the genomes of most gammaherpesviruses contain a large number of genes that are not directly linked to viral entry, replication, or morphogenesis (10, 15, 27, 31). The identification of additional herpesvirus proteins controlling the activation, differentiation, and survival of latently infected cells is of particular interest as these proteins constitute key components of gammaherpesvirus pathogenesis and a potential link to virus-associated oncogenic transformation.

We have used murine gammaherpesvirus 68 (MHV-68) as a molecular tool to gain further insights into the strategies employed by lymphotropic gammaherpesviruses to subvert B-cell function. MHV-68 uses B lymphocytes as the main target for long-term latent infection (13, 14, 26, 41). The establishment of latent states is characterized by a transient expansion of latently infected GC B cells in splenic follicles (14, 26, 33), followed by long-term latent infection in memory B cells (14, 41). As previously proposed for EBV (36), the infection of GC B cells by MHV-68 may constitute a strategy to expand the latently infected cell pool and gain access to long-lived memory B cells. If so, it can be speculated that MHV-68 proteins expressed during the establishment of latency in GC B cells are involved in subverting B-cell function (26). Recent studies suggest that M2 is probably one of such proteins. The gene encoding this protein is located near the 5' end of the MHV-68 genome (40). The M2 transcript is composed of two exons that, upon RNA splicing, produce a 192-amino-acid-long protein (17). An examination of its primary sequence indicates the presence of multiple proline-rich regions (PRRs) and potential phosphorylation sites. However, it bears no clear homology with other viral or eukaryotic proteins, suggesting that it may perform a unique function for the virus. Biochemical studies

* Corresponding author. Mailing address for J. Pedro Simas: Faculdade de Medicina, Avenida Professor Egas Moniz, 1649-028 Lisboa, Portugal. Phone: 351 21 799 9417. Fax: 351 21 799 9459. E-mail: psimas@fm.ul.pt. Mailing address for Xosé R. Bustelo: Centro de Investigación del Cáncer, CSIC-University of Salamanca, Campus Unamuno, E37007 Salamanca, Spain. Phone: 34-923294802. Fax: 34-923294743. E-mail: xbustelo@usal.es.

have shown that M2 inhibits interferon-mediated transcriptional activation by down-regulating STAT1/2 levels, suggesting that this protein may be involved in modulating the innate immunity of the host during the establishment of latency (22). Several other studies with mutant viruses showed that the absence of M2 results in reduced levels of acute splenic latency (16, 18, 24, 32). This deficit has been shown to be due to a decreased number of infected follicles rather than to an inability to expand the latent load in GC B cells (32). However, although M2 is required for an efficient colonization of splenic follicles, a lack of M2 leads to increased long-term levels of latency, predominantly in GC B cells (24, 32). This phenotype has been correlated with a deficit of latency in memory B cells (32).

The above findings are consistent with M2 playing a crucial role in the establishment of latency by signaling the cessation of the expansion of the viral load in GCs and by promoting the differentiation of latently infected GC B cells into long-lived memory B cells. Despite these advances, the molecular function of M2 remains largely unknown. An important step in that direction has been the discovery that M2 can associate with two members of the Vav oncoprotein family, Vav1 and Vav2 (25). Vav proteins are enzymes that promote GDP/GTP exchange on Rho/Rac proteins in a phosphorylation-dependent manner, thereby favoring the rapid transition of those GTPases from their inactive (GDP-bound) to active (GTP-bound) states during signal transduction (4). The activation of Rho/Rac proteins promotes extensive changes in intracellular pathways related to cytoskeletal change, mitogenesis, and cell survival (11). The interaction of M2 with Vav proteins was of particular interest to us since previous genetic evidence indicated that Vav proteins are crucial for the coordination of proper signaling responses in T- and B-cell lineages (37). To further characterize the interaction between M2 and Vav, in the present report we have analyzed the mechanistic aspects of that association, the possible effects of M2 on Vav signaling, and whether the manipulation of the Vav pathway was required for the function of M2 in MHV-68 latency. Our results indicate that M2 acts as a scaffold protein that, via PRRs and phosphotyrosine sequences, allows the assembly of a trimeric complex composed of M2, Vav proteins, and Src family members. The formation of this complex promotes the phosphorylation of Vav proteins and the activation of their exchange activity in both B cells and ectopic systems. Finally, the use of Vav family knockout animals demonstrates that the modulation of Vav activity is important for the establishment of latent infection of MHV-68 in GC B cells *in vivo*.

MATERIALS AND METHODS

Plasmids. M2 and mutants were amplified by PCR from MHV-68 genomic DNA. P to A and Y to F M2 mutants were generated by overlapping PCRs. PCR products were cloned into pCMV-HA/myc (Clontech), pMSCV-IRES-GFP (35), and pGEX-4T (Amersham Biosciences) for fibroblast, B-cell, and bacterial expression, respectively. The PCR-amplified mouse *vav2* cDNA was cloned into the pCMV-HA vector. Vav1, Vav1 Y174F, Vav1 (Δ 1-66), Rac1, and Rac1^{Q61L} expression plasmids have been described previously (8, 23, 30). The pGEX vector containing the PAK1 Rac binding domain (RBD) was provided by R. A. Cerione (Cornell University). Mouse cDNAs corresponding to Lyn and Fyn were provided by H. Murakami (Okayama University, Japan) and A. Shaw (Washington University School of Medicine), respectively, and subcloned into pCMV-HA. pMSCVK3-IRES-GFP was a gift from P. Stevenson (35). pEH1.4 has been described before (2).

Fusion proteins and immunological reagents. Glutathione *S*-transferase (GST) fusion proteins were expressed in *Escherichia coli* and purified according to standard procedures. The production of anti-M2 and -M3 antibodies has been previously described elsewhere (19, 25). Vav1 antibodies were obtained by immunizing rabbits with a GST-Vav1 DH fusion protein. Phosphospecific antibodies to Vav1 phospho-Y¹⁷⁴ were described before (23). Rabbit anti-Fyn and mouse anti-phosphotyrosine antibodies were purchased from Santa Cruz Biotechnology. Anti-hemagglutinin, AU5, and Myc antibodies were from Babco. Anti-GST and anti-actin antibodies were purchased from Sigma. CD45R/B220 antibodies (clone RA3-6B2) and the peanut agglutinin lectin were from BD Pharmingen and Vector Laboratories, respectively.

Tissue culture and DNA transfections. HEK 293T and COS1 cells were cultured in Dulbecco's modified Eagle's medium containing 10% fetal calf serum, 2 mM glutamine, and 100 U/ml of penicillin and streptomycin. A20 and S11 B-cell lines were cultured in RPMI supplemented as described above. For immunoprecipitation experiments, pull-down assays, and immunofluorescence microscopy, COS1 cells were transiently transfected with FuGENE 6 (Roche Molecular Biochemicals) according to the manufacturer's instructions. To detect Vav phosphorylation or Rac1 activation levels, COS1 cells were transfected using the DEAE-dextran method. B cells were transduced by the infection of A20 cells with supernatants derived from HEK 293T cells cotransfected with pMSCV-K3-IRES-GFP, pMSCV-M2-IRES-GFP, or pMSCV-M2P2-IRES-GFP retroviral vector and pEQPAM3 packaging vector. After 48 h of culture, green fluorescent protein-positive cells were purified by flow cytometry and cultured.

TranSignal SH3 domain array screen. Membranes (TranSignal; Panomics) were incubated with purified GST-M2 (50 μ g/ml). After extensive washing, positive interactions were detected by immunoblotting with the rabbit anti-M2 polyclonal serum.

Immunoprecipitation experiments. Transduced A20 (1×10^7) and normal S11 (5×10^7) cells were disrupted with ice-cold lysis buffer containing 10 mM Tris-HCl (pH 7.4), 100 mM NaCl, 0.5% Nonidet P-40 (Sigma), 1 mM NaVO₄ (Sigma), 1 mM NaF (Sigma), and a cocktail of protease inhibitors (C ϕ complete; Roche Molecular Biochemicals). COS1 cells were transiently transfected with expression plasmids carrying Vav1 (2 μ g), Vav2 (2 μ g), Fyn (2 μ g), and/or M2 (4 μ g), cultured for 48 h, and lysed as described above. Cleared supernatants were incubated with anti-M2, anti-Vav1, or anti-Fyn antibodies at 4°C for 2 h. Immune complexes were recovered by incubation with protein A-Sepharose beads (Amersham Biosciences) for 1 h at 4°C. After three washes with ice-cold lysis buffer, proteins were eluted in Laemmli's sample buffer, boiled, and resolved by sodium dodecyl sulfate-polyacrylamide gel electrophoresis. Immunoprecipitates were then analyzed by immunoblotting using appropriate antibodies.

Immunofluorescence analysis. COS1 cells grown on uncoated coverslips were transiently transfected with 1 μ g of the indicated plasmids. Thirty hours after transfection, cells were serum starved for 8 h and then incubated either with medium alone or with cytochalasin D (2 μ M, Sigma) for 30 min. Cells were then rinsed in phosphate-buffered saline (PBS) solution and fixed with 3.7% formaldehyde in PBS for 20 min. After three washes in PBS, cells were permeabilized by incubation for 10 min in PBS plus 0.1% Triton X-100 and then subjected to immunostaining with appropriate antibodies. F-actin was stained with rhodamine-labeled phalloidin (1:500 dilution; Molecular Probes). After three washes with PBS, coverslips were mounted onto microscope slides in the presence of Mowiol mounting medium.

Rac1 guanine nucleotide exchange assays. Rac1 stimulation *in vivo* was determined by GST-Pak1 RBD pull-down experiments. COS1 cells were transfected with expression plasmids carrying Rac1 (2 μ g), Vav1 (2 μ g), and/or M2 (4 μ g) in the indicated combinations. Transfected COS1 cells were lysed with ice-cold buffer containing 20 mM Tris-HCl (pH 7.6), 150 mM NaCl, 10 mM MgCl₂, 0.5% Triton X-100, 5 mM glycerophosphate (Sigma), 1 mM dithiothreitol (Sigma), and C ϕ complete. Cleared lysates were incubated for 90 min at 4°C with 10 μ g of a bacterially expressed GST fusion protein containing the PAK1 RBD previously immobilized onto glutathione-Sepharose beads. After incubation, beads were collected by centrifugation and washed three times with lysis buffer. Proteins were then eluted and denatured by boiling in Laemmli's sample buffer and analyzed by immunoblotting.

In vitro kinase assays. COS1 cells were transfected with expression plasmids carrying Vav1 (2 μ g), Fyn (2 μ g), and/or M2 (4 μ g). Transfected cells were lysed on ice-cold lysis buffer containing 10 mM Tris-HCl (pH 7.4), 100 mM NaCl, 0.5% Nonidet P-40, 100 μ M NaVO₄, 1 mM NaF, and C ϕ complete. The drugs PP2 and PP3 (Calbiochem) were added to the lysis buffer at a final concentration of 10 μ M when required. Cleared lysates were incubated for 2 h at 4°C with anti-Vav1 antibodies. Immunocomplexes were collected with protein A-Sepharose beads and washed twice in lysis buffer and once in kinase buffer (20 mM HEPES-KOH (pH 7.2) and 10 mM MgCl₂). Immunocomplexes were incubated at room tem-

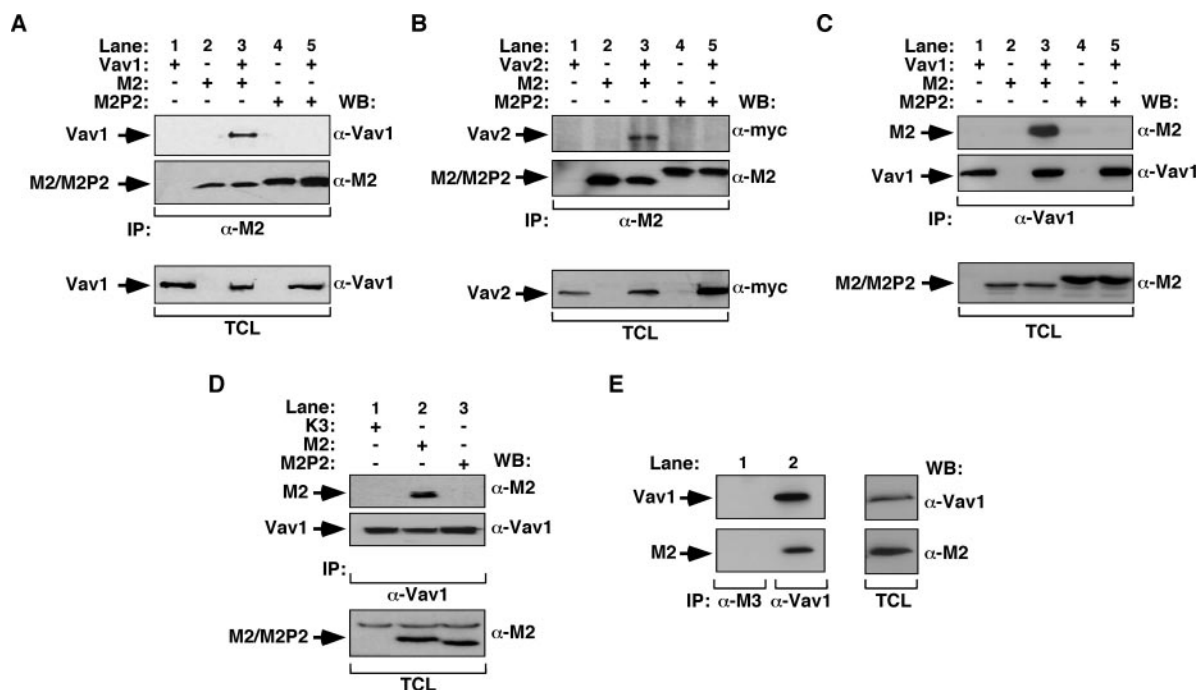


FIG. 1. M2 coimmunoprecipitates with Vav1 and Vav2 proteins in vivo. (A to C) COS1 cells were transiently transfected with combinations of plasmids encoding the indicated proteins (top). After lysis, total cell extracts were obtained and immunoprecipitated with either anti-M2 (A and B) or anti-Vav1 (C) antibodies. After appropriate washes, the immunoprecipitates were analyzed by Western blotting using anti-Vav1 (A, upper panel), anti-Myc (B, upper panel), or anti-M2 (C, upper panel) antibodies. Filters were subsequently reblotted with either anti-M2 (A and B, second panels from the top) or anti-Vav1 (C, second panel from the top) antibodies. In addition, representative aliquots of the total cellular lysates utilized above were used to detect the expression of Vav1 (A, bottom panel), Vav2 (B, bottom panel), and M2 proteins (C, bottom panel). (D) Cellular lysates from A20 B cells ectopically expressing the indicated proteins (top) were immunoprecipitated with anti-Vav1 antibodies. The immunoprecipitates were analyzed by Western blotting using anti-M2 (upper panel) and then reblotted with anti-Vav1 (second panel from the top). Aliquots of the total cellular lysates were used to detect the expression of the indicated M2 proteins (third panel from the top). (E) Cellular lysates from S11 cells were immunoprecipitated with anti-M3 or anti-Vav1 antibodies. The resulting immunoprecipitates were analyzed by Western blotting using either anti-Vav1 (first panel from the top) or anti-M2 (second panel from the top). Representative aliquots of total cellular lysates were used to detect the expression of Vav1 and M2 in this cell line (right panel). -, without; +, with; α, anti; IP, immunoprecipitation; TCL, total cellular lysates; WB, Western blotting.

perature for 30 min in kinase buffer with 2.5 μCi [γ - 32 P]ATP and 1 μM ATP. Reactions were stopped by adding 1 ml of a buffer containing 10 mM Tris-HCl (pH 8.0), 150 mM NaCl, 2 mM EDTA, and 0.2% Nonidet P-40. Beads were collected by centrifugation and washed three times in lysis buffer. After separation by sodium dodecyl sulfate-polyacrylamide gel electrophoresis, proteins were fixed, dried, and subjected to autoradiography.

Prediction of phosphorylation sites. The identification of the possible phosphorylation sites of M2 was performed using the NetPhos 2.0 software available at <http://www.cbs.dtu.dk/services/NetPhos>.

Analysis of MHV-68 lytic and latent infection in *vav*-deficient mice. *vav1*^{-/-} and *vav2*^{-/-} mice were generously provided by V. Tybulewicz and M. Turner, respectively. MHV-68 working stocks were prepared as previously described (32). Wild-type and knockout mice were inoculated intranasally at 6 to 8 weeks of age with 10⁴ PFU of MHV-68 in 20 μl PBS under halothane anesthesia. At 3, 5, 7, 14, 21, and 50 days after infection, lungs or spleens were removed and processed for subsequent analysis. Infectious virus titers in freeze-thawed lung and spleen homogenates were determined by suspension assays using BHK-21 cells. The presence of latent viruses was checked using explant cocultures of single-cell suspension splenocytes with BHK-21 cells. Plates were incubated for 4 (suspension assay) or 5 (coculture assay) days, fixed with 10% formal saline, and counterstained with toluidine blue. Viral plaques were counted with a plate microscope. The frequency of MHV-68 genome-positive cells was determined for the population of flow cytometry-purified splenic GC B cells (B220⁺ PNA^{high}) by limiting dilution combined with real-time PCR, as previously described (32). The purity of sorted populations was always >95% as analyzed by flow cytometry. For in situ hybridization, digoxigenin-labeled riboprobes corresponding to MHV-68 microRNAs (miRNAs) 1 to 4 were generated by T7 transcription of pEH1.4 and

used as previously indicated (33). Probes were generated using a commercial kit from Roche Molecular Biochemicals.

RESULTS

Interaction of M2 with Vav proteins. Recently, we described the identification of Vav1 and Vav2 proteins as M2 partners using two-hybrid system screenings (25). These experiments also indicated that the interaction between M2 and Vav proteins was mediated by the recognition of three M2 PRRs located at positions 162 to 165, 167 to 170, and 174 to 176 of the most C-terminal SH3 domain of Vav proteins (25). In agreement with these data, coimmunoprecipitation experiments conducted in COS1 cells demonstrated that the full-length Vav1 and Vav2 proteins can interact with M2 but not with an M2 mutant (referred to hereafter as M2P2), in which the proline residues at positions 165, 167, 170, and 174 were replaced by alanine residues (Fig. 1A to C). To further confirm the physical interaction between M2 and Vav proteins in a more relevant biological context, we tested whether M2 and Vav1 could coimmunoprecipitate in a B-lymphocyte-derived cell line. To this end, we transduced A20 B cells with recom-

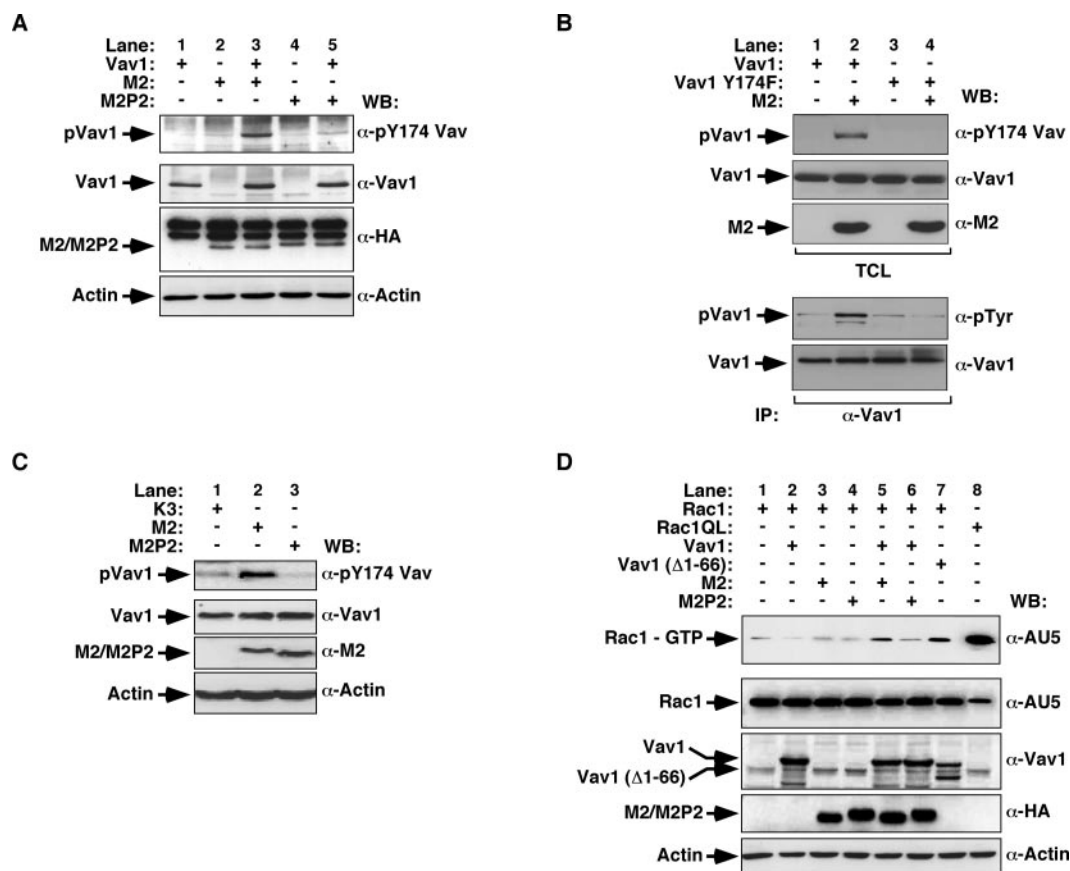


FIG. 2. M2 promotes Vav1 activation. (A, B, and C) M2 induces Vav1 phosphorylation. Total cellular lysates or Vav1 immunoprecipitates obtained from COS1 cells (A and B) or retrovirally infected A20 B cells (C) expressing the indicated combinations of proteins were subjected to immunoblot analysis using the indicated antibodies (A, B, and C, right side of panels). (D) M2 promotes Rac1 activation in a Vav1-dependent manner. Upper panel, total cellular lysates obtained from COS1 cells expressing the indicated combinations of proteins (top) were subjected to GST-Pak1 pull-down experiments. Lower panels, aliquots from the total cellular lysates used above were analyzed with the indicated antibodies (right side) to detect the expression of the indicated protein after the transfections. -, without; +, with; α, anti; IP, immunoprecipitation; TCL, total cellular lysates; WB, Western blotting.

binant retroviruses encoding either wild-type M2 or the M2P2 mutant. Total cell lysates were obtained and immunoprecipitated with an anti-Vav1 serum. The presence of M2 protein in each of these immunoprecipitates was finally assessed by immunoblot analysis using anti-M2 antibodies. Under these conditions, the endogenous Vav1 protein could associate with wild-type M2 but not with the M2P2 mutant protein (Fig. 1D, upper panel, compare lanes 2 and 3). As an additional negative control, Vav1 could not associate with K3, an MHV-68-encoded protein that is structurally unrelated to M2. Further immunoblotting confirmed that Vav1 and M2 proteins were present at comparable levels in the appropriate samples (Fig. 1D, second and third panels from the top). Similar coimmunoprecipitation experiments indicated that M2 and Vav1 could also coimmunoprecipitate in S11 cells (Fig. 1E), a murine B-cell lymphoma-derived cell line latently infected with MHV-68 (38). The use of an unrelated antibody to the viral M3 protein yielded no Vav1 or M2 coimmunoprecipitation (Fig. 1E). These results indicate that M2 can interact efficiently with Vav1 in the physiological context of infection as well as in ectopic systems such as COS1 cells.

M2 promotes the phosphorylation and catalytic activation of Vav1. The interaction between M2 and Vav1 suggested that this exchange factor could be one of the intracellular targets of M2. Therefore, we speculated that the expression of M2 could alter the regulatory loop of Vav1 during cell signaling, resulting in either up- or down-modulation of its normal biological activities. It has been clearly established that the key regulatory step of Vav proteins is the modulation of their catalytic activities by direct phosphorylation on a specific tyrosine residue (Y¹⁷⁴) (3). Based on these previous observations, we decided to test whether the expression of M2 could alter the phosphorylation levels of Vav1. To this end, we expressed Vav1 alone and in combination with either wild-type M2 or the M2P2 mutant in COS1 cells. After 48 h of culture, the levels of phosphorylation of Vav1 on Y¹⁷⁴ were determined by immunoblotting of total cellular lysates with a previously described antibody that specifically recognizes this phosphorylated residue (23). We observed that Vav1 becomes highly phosphorylated on Y¹⁷⁴ when coexpressed with wild-type M2 (Fig. 2A, upper panel, compare lanes 1 and 3). This is a specific effect since little phosphorylation of Vav1 is observed when ex-

pressed either alone or in the presence of the M2P2 mutant (Fig. 2A, upper panel). No detectable phosphorylation of Vav1 is induced by M2 when the wild-type version of this guanine nucleotide exchange factor (GEF) is replaced by a mutant version lacking residue Y¹⁷⁴ (Y174F) (23), indicating that M2 triggers a specific phosphorylation of Vav1 in this key regulatory tyrosine residue and not in other potential phosphorylation sites located throughout the rest of the Vav1 molecule (Fig. 2B). The effect of M2 on Vav1 phosphorylation is also conserved in B cells since the expression of M2 in the A20 B-cell line leads to a reproducible enhancement of Vav1 phosphorylation on the Y¹⁷⁴ residue (Fig. 2C, upper panel). As in the case of COS1 cells, this effect is specific for the wild-type M2 because the expression of either the M2P2 mutant protein or the unrelated K3 protein does not alter the phosphorylation levels of this GEF (Fig. 2C, upper panel). Immunoblotting experiments confirmed that all of these proteins were appropriately expressed (Fig. 2A to C). These observations indicate that M2 promotes Vav1 tyrosine phosphorylation in an antigen- and extracellular stimulus-independent manner in B lymphocytes and COS1 cells, respectively.

Since the phosphorylation of Vav1 on Y¹⁷⁴ results in the stimulation of its exchange activity towards Rho/Rac proteins (3), we tested the effect of M2 overexpression on the activation levels of Rac1 *in vivo*. To this end, we transfected COS1 cells with a plasmid encoding an AU5-tagged version of wild-type Rac1 either alone or with the presence of the indicated combinations of Vav1- and M2-encoding vectors. As a positive control, we transfected cells with plasmids encoding the constitutively active versions of either Rac1 (Rac1^{Q61L} point mutant) or Vav1 (Δ 1-66 deletion mutant) (4). The activation levels of Rac1 under these conditions were subsequently determined by pull-down experiments with a GST protein fused to the Rac1 binding domain of Pak1 (Pak1 RBD). The coexpression of M2 and Vav1 resulted in high levels of Rac1 activation comparable to those obtained upon expression of the *vav1* oncogene (Fig. 2D, upper panel, compare lanes 5 and 7). Such activation was dependent on the interaction between M2 and Vav1 because no stimulation of Rac1 could be observed when Vav1 was expressed with the M2P2 mutant (Fig. 2D, upper panel, lane 6). Likewise, no changes in Rac1 activation could be observed in cells expressing wild-type M2 without Vav1 (Fig. 2D, upper panel, lane 3). Immunoblot analysis confirmed that all of the proteins used were expressed at equal levels in the appropriate transfections (Fig. 2D, lower panels). Taken together, these experiments demonstrate that M2 mediates the activation of Vav proteins by inducing the phosphorylation of the key regulatory Y¹⁷⁴ site. Furthermore, the lack of effect of the M2P2 mutant indicates that Vav1 activation requires the stable association of this GEF to the C-terminal M2 PRR.

M2 and Vav1 colocalize in the juxtamembrane area of mammalian cells. We next conducted immunofluorescence experiments to analyze the distribution of M2 within cells and its possible colocalization with Vav1. We used COS1 cells in these studies because their large cytoplasm facilitated a better discrimination of cytosolic and membrane structures in the subcellular localization experiments. When expressed alone, hemagglutinin (HA)-M2 was found to localize mainly in the nucleus of the transfected cells (Fig. 3A, panel a). HA-M2 was

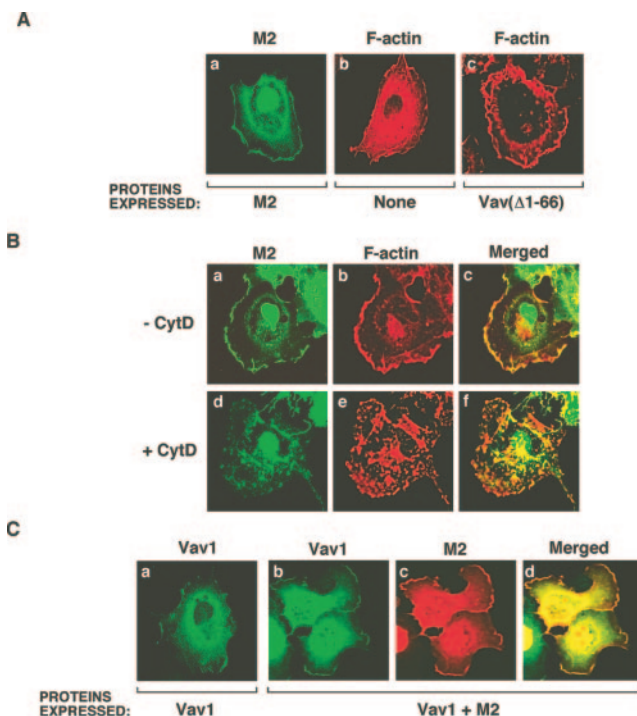


FIG. 3. Subcellular colocalization of M2 and Vav1. (A) Subcellular localization of M2 in COS1 cells. Serum-starved COS1 cells were transiently transfected with the indicated proteins (bottom) and subjected to immunofluorescence analysis after staining with either anti-HA antibodies (panel a, green) or rhodamine-phalloidin (panels b and c, red). (B) Effect of cytochalasin D on the subcellular localization of M2. Quiescent cells expressing HA-M2 (panels a through f) were left untreated (–CytD) or treated (+CytD) with cytochalasin D as described in Materials and Methods. Cells were then double stained with anti-HA and rhodamine-phalloidin. The subcellular localization of M2 and F-actin is seen in green (panels a, c, d, and f) and red (panels b, e, and f), respectively. The areas of colocalization of M2 and F-actin are seen in yellow (panels c and f). (C) Quiescent cells expressing the indicated combinations of Vav1 and HA-M2 proteins (bottom) were subjected to immunofluorescence analysis after staining with anti-Vav1 (panels a to d) and anti-HA (panels b to d) antibodies. The localization of Vav1 and M2 in each condition is seen in green (panels a, b, and d) and red (c and e), respectively. The areas of colocalization are in yellow (panel d).

also found highly enriched in membrane ruffles (Fig. 3A, panel a). Interestingly, an increase in membrane ruffling was consistently observed in HA-M2-transfected cells (Fig. 3A, compare panels a and b), suggesting that the expression of M2 promotes cytoskeletal rearrangements in the target cells. These ruffles were less pronounced than those observed with well-established cytoskeletal organizers, such as Vav1 oncoproteins or activated Rac1 (Fig. 3A, panel c; also data not shown). The correlation between M2 and the cell cytoskeleton was further demonstrated by dual fluorescence experiments, which show high levels of colocalization between M2 and F-actin in transfected cells (Fig. 3B, upper panels). In order to further explore the interaction of M2 with F-actin, we investigated the effect of the F-actin-disrupting agent cytochalasin D on the subcellular localization of M2. As previously described (6), the incubation of COS1 cells with this drug induces the initial collapse of F-actin filaments into cytoplasmic clusters (Fig. 3B, panel e). Under

these culture conditions, M2 showed an identical behavior to F-actin, losing its localization at the juxtamembrane areas and moving into F-actin cytoplasmic clusters (Fig. 3B, lower panels). Thus, the distribution of the M2 juxtamembrane pool is probably due to its association with cytoskeletal components rather than a consequence of its direct interaction with the plasma membrane.

When expressed alone, Vav1 showed a uniform distribution in the cytoplasm of transfected cells, with occasional enrichment in areas of membrane ruffling (Fig. 3C, panel a). We could not observe any significant change in the subcellular localization of M2 when these two proteins were coexpressed (Fig. 3C, panel c). In contrast, more Vav1 was found localized at membrane ruffles upon coexpression with M2 (Fig. 3C, panel b). In this case, a strong colocalization between M2 and Vav1 was also observed in peripheral membrane ruffles (Fig. 3C, panel d). The importance of these results is fourfold. Firstly, they show that M2 has two different subcellular localizations, one present in the nucleoplasm and the other one in close proximity to the plasma membrane. Secondly, they suggest that the localization of M2 in membrane ruffling areas is due to its interaction with the F-actin cytoskeleton. Thirdly, they demonstrate that the juxtamembrane M2 pool, but not its nuclear-localized fraction, is involved in the interaction with Vav1. Finally, they suggest that M2 promotes a translocation of Vav1 to F-actin-enriched areas of the cell, which is in good agreement with its ability to stimulate the enzyme activity of this Rho/Rac GEF.

M2 is a scaffold protein that facilitates the phosphorylation of Vav proteins by Src family kinases. As an initial approach to identifying the kinase involved in the M2-dependent phosphorylation of Vav1, we screened filters containing SH3 domains from 108 proteins with a GST-M2 fusion protein probe (see Materials and Methods). We found that M2 could bind to 24 of those SH3 domains (Table 1). Those regions belonged to adaptor proteins (Grb2-like adaptor proteins, Nck, and Spin90), synaptic molecules (endophilin and PSD95), cytoskeletal-related molecules (CASK, Cip4, cortactin, HS1, and BPAG1), Vav family proteins (Vav1 and Vav2), an additional Rho/Rac exchange factor (RGNEF-6), and a number of protein tyrosine kinases (Hck, Fyn, Lyn, Yes, TXK, and Fgr) (Table 1). Sequence analyses of these domains revealed no recognizable consensus sequences that could determine the specific recognition of the viral protein (data not shown). To investigate whether the M2-dependent phosphorylation of Vav1 could be mediated by some of those Src family kinases, we evaluated the ability of Lyn and Fyn to enhance the M2-mediated phosphorylation of Vav1 using coexpression experiments in COS1 cells. These experiments demonstrated that the expression of Vav1 with M2 and Fyn resulted in higher phosphorylation levels of Vav1 than those obtained when coexpressed with M2 alone (Fig. 4A, upper panel, compare lanes 3 and 9). Lyn also induced higher phosphorylation levels of Vav1, although at significantly lower levels than Fyn did (Fig. 4A, upper panel, compare lane 6 with lanes 3 and 9). Immunoblot analysis confirmed that all proteins were properly expressed in the respective samples (Fig. 4A, lower panels).

In order to check whether the enhanced phosphorylation of Vav1 induced by Fyn required the formation of a stable complex, we investigated whether this kinase could be detected in

Vav1 immunoprecipitates. For this purpose, we expressed Fyn, Vav1, M2, and M2P2 proteins in the indicated combinations and, after immunoprecipitation with anti-Vav1 antibodies, tested the presence of the kinase using anti-Fyn immunoblots (Fig. 4B). These experiments indicated that Vav1 associates with Fyn when coexpressed with wild-type M2 (Fig. 4B, upper panel, lane 6). Such association does not occur when Vav1 is expressed either without M2 or with the M2P2 mutant (Fig. 4B, upper panel, lanes 5 and 7), indicating that the Vav1/Fyn interaction occurs only in the presence of M2. In contrast to these results, Fyn was totally dispensable for the M2/Vav1 interaction (Fig. 4B, second panel from the top, lanes 3 and 6). Similar results were obtained when the formation of this trimeric complex was tested in A20 B cells. As shown in Fig. 4C, endogenous Vav1 coimmunoprecipitates with endogenous Fyn only when M2 is expressed in cells (compare lanes 1 and 2). Interestingly, Fyn could also coimmunoprecipitate with a small fraction of the M2P2 protein without detectable levels of Vav1 (Fig. 4C, first and second panels from the top). These results indicate that Vav1 and Fyn use no overlapping docking sites. Furthermore, the coimmunoprecipitation of M2P2 with Fyn suggests that this association is not totally dependent on the interaction between SH3 and PRR detected in the filter assays (see above) (Table 1), indicating the probable presence of additional docking sites in the molecule.

In vitro kinase assays performed with anti-Vav1 immunoprecipitates confirmed that Fyn can phosphorylate Vav1 and, in addition, M2 (Fig. 4D, lane 6, and E, lane 4). A small but detectable kinase activity was also found in the Vav1/M2 complex lacking Fyn, suggesting the presence of an endogenous tyrosine kinase in those immunoprecipitates (Fig. 4D, lane 3, and E, lane 3). Both kinase activities were eliminated when M2 was replaced by the M2P2 mutant in those transfections (Fig. 4D, lanes 7 and 4). Moreover, no kinase activity was observed in anti-Vav1 immunoprecipitates obtained from mock-transfected cells or cells expressing Vav1 alone (Fig. 4D and E, lanes 1 and 2). The phosphorylation of Vav1 and M2 in those immunocomplexes was due to Fyn and not to other associated kinases since the addition of the Src family inhibitor PP2 totally blocked such a phosphorylation event (Fig. 4E, lanes 6 and 7). An inactive compound analogous to PP2 (PP3) did not affect such phosphorylation (Fig. 4E, lanes 3 and 4). Taken collectively, these results suggest that M2 triggers the phosphorylation and activation of Vav1 by favoring the formation of a trimeric complex with Src family members. In addition, they indicate that M2 is also a phosphorylation substrate for the associated tyrosine kinase.

Two tyrosine residues localized at positions 127 and 136 of M2 are important for the interaction with Fyn and Vav1. The examination of the primary sequence of M2 indicates the presence of only three tyrosine residues at positions 40, 127, and 136. Two of those residues (127 and 136) are within amino acid sequences that are consensus for recognition by tyrosine kinases, suggesting that they are probably the phosphorylation targets of Fyn. To verify this hypothesis, we generated an M2 mutant protein (referred to hereafter as M2Y protein) in which these two tyrosine residues were simultaneously mutated to phenylalanine. This mutant protein could not become phosphorylated in in vitro kinase experiments when tested in the presence of Fyn and ^{32}P -labeled ATP, indicating that these two

TABLE 1. GST-M2 binding to SH3 domains from human proteins

SH3 domains present in ^a :		
Array I	Array II	Array III
Amphiphysin	Abl interactor protein 2	Arginine <i>N</i> -methyltransferase 2
Discs large homolog 2	Phosphatidylinositol 3-kinase regulatory alpha subunit	Growth factor receptor-bound protein 2, SH3 domain 1
Vav1 proto-oncogene, SH3 domain 1	GRB2-related adaptor protein, SH3 domain 1	Myosin-IE
Beta-lymphocyte-specific protein tyrosine kinase	Vav2 protein, SH3 domain 1	SH3 protein interacting with Nck, 90 kDa
Human T-lymphocyte-specific protein tyrosine kinase p56 LCK	Grb2-related adaptor protein 2, SH3 domain 1	Grb2-related adaptor protein 2, SH3 domain 1
55-kDa erythrocyte membrane protein	Channel-associated protein of synapse 110	Grb2-D2 growth factor receptor-bound protein 2, SH3 domain 2
Cytoplasmic protein NCK1, SH3 domain 3	c-Jun-amino-terminal kinase interacting protein 1	MYIF myosin-IF
Abelson tyrosine kinase	Vav3 protein, SH3 domain 1	Triple functional domain protein
Spectrin alpha chain (nonerythrocytic)	Abelson-related protein, Arg	Bullous pemphigoid antigen
Cellular Gardner-Rasheed feline sarcoma virus protein	Stac protein	Grb-2 related adaptor protein 2, SH3 domain 2
PAK-interacting exchange factor beta	Mitogen-activated protein kinase kinase 10	Neutrophil oxidase factor (p47-phox) (47-kDa), SH3 domain 1
Phospholipase C gamma-1	Vav3 protein, SH3 domain 2	VINE-D2 vinexin, SH3 domain 2
Cortactin	Dihydropyridine-sensitive L-type, calcium channel beta-1 subunit	Voltage-dependent calcium channel beta-2 subunit
Proto-oncogene tyrosine protein kinase FYN		Intersectin 1, SH3 domain 3
Peroxisomal membrane protein PEX13	Tyrosine protein kinase Tec	Neutrophil oxidase factor (p47-phox) (48-kDa), SH3 domain 2
Retinoblastoma protein-interacting zinc-finger	Myosin VIIa	Cellular Rous sarcoma viral oncogene homolog
Mixed-lineage kinase 3	Vinexin, SH3 domain 1	Proto-oncogene CRK, SH3 domain 1
Nebulin	CRK-like protein, SH3 domain 1	Intersectin 1, SH3 domain 4
Bruton tyrosine kinase	Cdc42-interacting protein 4	Cytoplasmic protein NCK2, SH3 domain 1
Phosphoinositide 3-kinase regulatory beta subunit	Cytoplasmic protein NCK2, SH3 domain 2	Proto-oncogene CRK, SH3 domain 2
Yamaguchi sarcoma virus oncogene homolog 1	Vinexin, SH3 domain 3	c-Jun-amino-terminal kinase interacting protein 2
Cellular Rous sarcoma viral oncogene homolog	Peripheral plasma membrane protein CASK	Juvenile nephronophthisis protein
Ras GTPase-activating protein 1	1-Phosphatidylinositol-4,5-bisphosphate phosphodiesterase gamma 2	Crk-like protein, SH3 domain 2
Intersectin, SH3 domain 1		Ick/yes-related novel (LYN) protein tyrosine kinase
Abelson-related protein, Arg	Cytoplasmic protein NCK2, SH3 domain 3	Otoraplin
Fyn binding protein, SH3 domain 1	Cellular Rous sarcoma viral oncogene homolog	FYN-binding protein, SH3 domain 2
Presynaptic density protein 95	Cytoplasmic protein NCK1, SH3 domain 2	Zonula occludens 2 protein
Intersectin 1, SH3 domain 2	Rho guanine nucleotide exchange factor 6	Synapse-associated protein 97 (SAP97)
Spectrin alpha chain, erythrocyte	Rho-GTPase-activating protein 4	GTPase-activating protein
Hemopoietic cell kinase	Presynaptic protein SAP102	Megakaryocyte-associated tyrosine protein kinase
Rho guanine nucleotide exchange factor (GEF) 5	CRK-associated substrate	SH3-containing GRB2-like protein 2
Tyrosine protein, kinase TXK	SH3-containing GRB2-like protein 1	Grb2-related adaptor protein, SH3 domain 2
Interleukin-2-inducible T-cell kinase	Neutrophil cytosol factor 2, SH3 domain 2	Melanoma inhibitory activity
Vav2 oncogene product, SH3 domain 2	Myc box-dependent interacting protein 1	SH3-containing GRB2-like protein 3
Hematopoietic-specific protein 1	Sorting nexin 9	
Avian sarcoma virus CT10 oncogene homolog, SH3 domain 2	Osteoclast stimulating factor 1	
Neurite outgrowth factor or neutrophil cytosol factor 2, SH3 domain 1	Embryonal Fyn-associated substrate	
Signal-transducing adaptor molecule	UBASH3	

^a SH3 domains that bound to GST-M2 are shown in bold type.

residues are indeed the sites phosphorylated by this kinase (data not shown). To investigate the functional roles of these two tyrosine residues, we investigated their roles in modulating the association of M2 with its intracellular targets. To this end, we first evaluated the effects of the described mutant on M2

phosphorylation and Fyn association using coimmunoprecipitation experiments in COS1 cells. When expressed alone, wild-type M2 showed significant levels of tyrosine phosphorylation (Fig. 5A, upper panel, lane 1). This phosphorylation was not observed when the M2Y and the M2P2 mutant proteins were

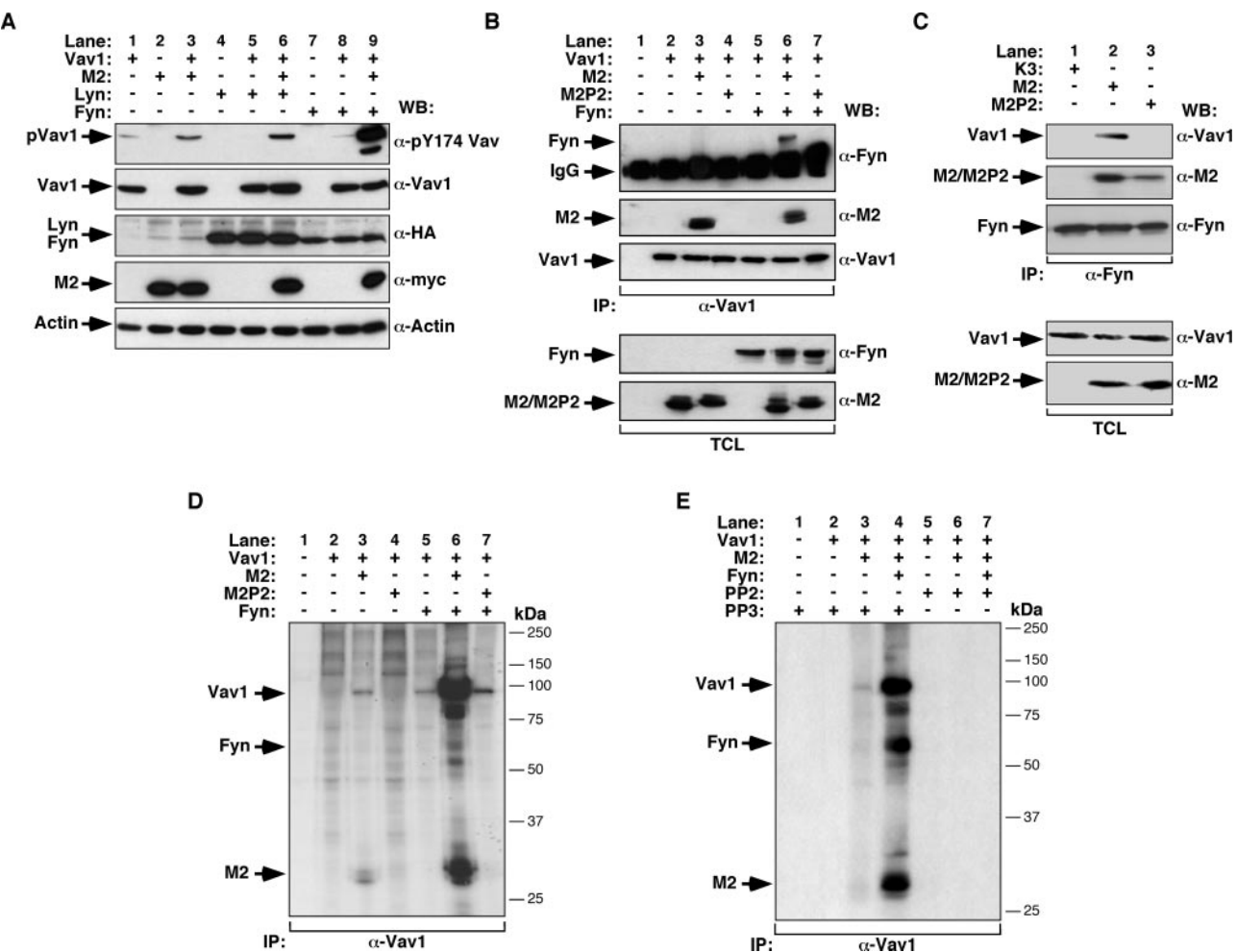


FIG. 4. M2 mediates Vav1 phosphorylation via Src family kinases. (A and B) Total cellular lysates obtained from COS1 cells expressing the specified combinations of proteins (top) were either immunoblotted (A) or immunoprecipitated (B) using anti-Vav1 antibodies. Samples were analyzed by Western blotting using the indicated antibodies (right side of the panels). In panel B, representative aliquots of total cellular lysates were used to detect the expression of Fyn (fourth panel from the top) and M2 proteins (fifth panel from the top). (C) Cellular extracts from A20 B cells expressing the indicated proteins (top) were immunoprecipitated with anti-Fyn antibodies. After transfer to nitrocellulose filters, samples were analyzed by Western blotting using the indicated antibodies (right side of the panels). Aliquots of total cellular lysates were used to detect the expression of Vav1 (fourth panel from the top) and M2 proteins (fifth panel from the top). (D and E) COS1 cell lysates containing the indicated combination of ectopically expressed proteins (top) were immunoprecipitated with anti-Vav1 antibodies and subjected to immunocomplex kinase assays in the absence (D) or presence (E) of the chemicals PP2 and PP3 (10 μ M each). The mobilities of Vav1, Fyn, and M2 are indicated by arrows. Molecular mass markers are indicated on the right. -, without; +, with; α , anti; IP, immunoprecipitation; TCL, total cellular lysates; WB, Western blotting.

expressed alone (Fig. 5A, upper panel, lanes 2 and 3). The coexpression of Fyn led to an enhancement in the phosphorylation levels of M2 and at significantly lower levels of M2P2 (Fig. 5A, upper panel, lanes 4 and 5). However, the M2Y protein remained unphosphorylated under these conditions (Fig. 5A, upper panel, lane 6). Interestingly, these anti-phosphotyrosine immunoblots revealed that autophosphorylated Fyn also coimmunoprecipitated with wild-type M2 (Fig. 5A, upper panel, lane 4). However, this interaction was significantly decreased in the case of the M2P2 mutant and, to a much larger extent, in the case of the M2Y protein (Fig. 5A, upper panel, lanes 5 and 6). The changes in the affinity of the interaction of Fyn with the M2 mutants were corroborated using anti-Fyn immunoblots of the same filters, which show only significant detectable levels of Fyn in the immunoprecipi-

tates containing wild-type M2 (Fig. 5A, second panel from the top). These differences in association were not due to different expression levels since all M2 proteins were immunoprecipitated at comparable levels in all of the experimental conditions (Fig. 5A, third panel from the top). Levels of Fyn expression were also similar in the appropriate transfections (Fig. 5A, fourth panel from the top). Using a similar approach, we observed that the M2Y mutation also reduced the levels of interaction of M2 with Vav1 (Fig. 5B, upper panel). However, this effect was less dramatic than the mutation of the C-terminal PRR because M2Y, unlike the M2P2 protein, could still be detected in the anti-Vav1 immunoprecipitates (Fig. 5B, upper panel, lane 4). The coimmunoprecipitation of Fyn with Vav1 was also eliminated when wild-type M2 was substituted by its M2Y mutant in the coexpression experiments (Fig. 5B, second

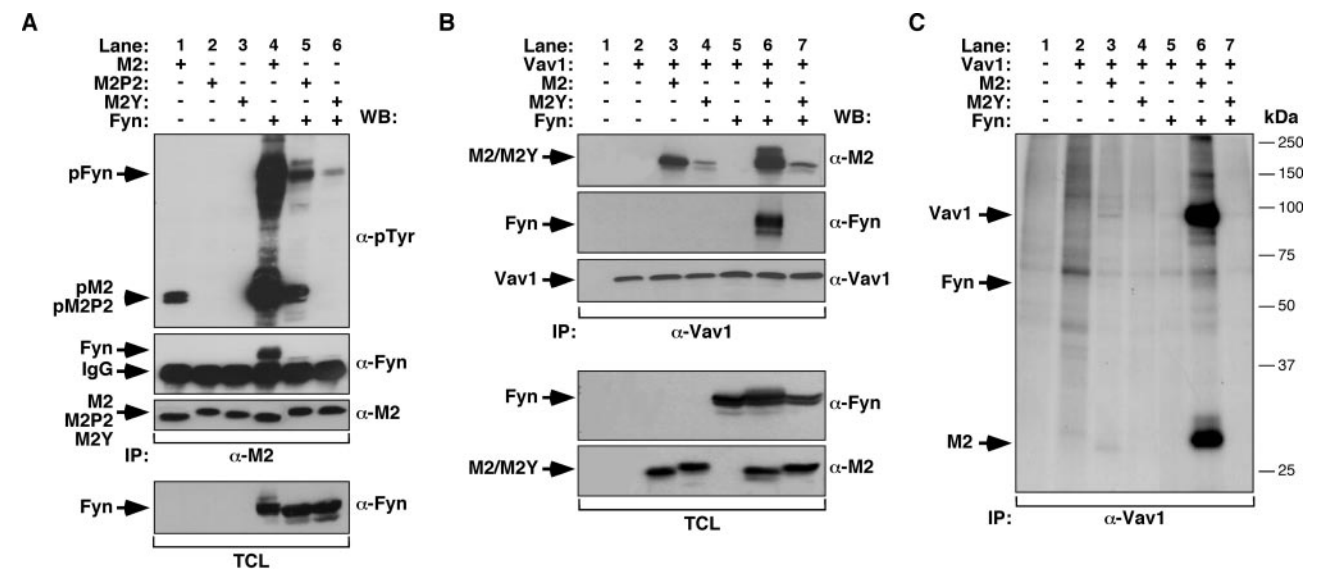


FIG. 5. M2 phosphorylation is necessary for the M2-dependent phosphorylation of Vav1. (A and B) COS1 cells transiently transfected with plasmids encoding the indicated proteins (top) were lysed, and the cellular extracts obtained were incubated with either anti-M2 (A) or anti-Vav1 (B) antibodies. Immunoprecipitates were then analyzed by Western blotting using the indicated antibodies (right side of panels). Representative aliquots of the total cellular lysates (TCL) were also analyzed by immunoblotting to detect the expression of the indicated proteins. (C) Cellular extracts derived from COS1 cells expressing the indicated combinations of proteins (top) were immunoprecipitated with anti-Vav1 antibodies and subjected to *in vitro* kinase reactions as described in Materials and Methods. The mobilities of Vav1, Fyn, and M2 are indicated by arrows. The position of molecular mass markers is indicated on the right. –, without; +, with; α , anti; IP, immunoprecipitation; WB, Western blotting.

panel from the top, lane 7). Additional immunoblots confirmed that Vav1, Fyn, and all of the M2 proteins were expressed at similar levels in COS1 cells (Fig. 5B, third, fourth, and fifth panels from the top, respectively). In agreement with these results, *in vitro* kinase assays demonstrated that the kinase activity associated with the Vav1/M2 complex was totally lost when Vav1 was coexpressed with the M2Y mutant (Fig. 5C, compare lanes 6 and 7). These observations indicate that the phosphorylation of M2 at positions Y¹²⁷ and Y¹³⁶ is an essential step for the assembly of a trimolecular complex with Fyn and Vav1. In addition, they suggest that these phosphotyrosine sequences have a higher hierarchical position in this signaling event than that of the PRR because M2 proteins with intact PRRs cannot mediate the phosphorylation of Vav1 in the absence of these two tyrosine residues.

Vav proteins are required for the normal establishment of latent infection of B cells by MHV-68. To evaluate the biolog-

ical significance of the interaction of M2 with Vav proteins during latent infection, we finally tested the influence that the disruption of either *vav1* or *vav2* genes has on establishment of the latency of MHV-68 in the host GC B cells. To this end, we infected mice of the indicated genotypes with wild-type MHV-68 via the intranasal route and, at the indicated time points, quantified the number of splenic B cells with MHV-68 genomes. No differences were observed in the number of viral genome-positive GC B cells at postinfection day 14 in any of those animals (Table 2). In contrast, after longer postinfection periods (50 days), both *vav1*- and *vav2*-deficient animals showed 100-fold-higher frequencies of MHV-68-positive B cells compared with those of wild-type animals (Table 2). These results are comparable to those obtained when wild-type mice are infected with an MHV-68 viral mutant lacking the M2 protein (32). We next investigated whether the deficiency in either Vav1 or Vav2 protein function could compromise the

TABLE 2. Reciprocal frequency of MHV-68 infection in GC B cells in *vav1*- and *vav2*-deficient mice^a

Days postinfection	Mice	Reciprocal frequency ^b of viral DNA-positive cells	% Purity ^c	% Cells ^d	Total no. of cells ^e	No. of viral DNA-positive cells ^f
14	wt	158 (96–434)	99.5	2.4	4.8 × 10 ⁶	30,380
	<i>vav1</i> ^{−/−}	93 (60–208)	98.4	4.9	9.8 × 10 ⁶	105,376
	<i>vav2</i> ^{−/−}	46 (28–125)	99.1	4.0	8 × 10 ⁶	173,913
50	wt	1,093 (697–2,532)	95.8	2.1	4.2 × 10 ⁶	3,843
	<i>vav1</i> ^{−/−}	10 (7–26)	97.0	2.4	4.8 × 10 ⁶	480,000
	<i>vav2</i> ^{−/−}	5 (3–11)	95.9	2.1	4.2 × 10 ⁶	840,000

^a Data were obtained from pools of at least five spleens. wt, wild type.
^b Frequencies were calculated by limiting-dilution analysis with 95% confidence intervals (numbers in parentheses).
^c The purity of sorted cells was determined by fluorescence-activated cell sorting (FACS) analysis.
^d The percentage of each population of total spleen was determined by FACS analysis.
^e The total number of cells was estimated from the percentage of the total spleen, based on an estimate of 2 × 10⁸ cells/spleen.
^f The number of latently infected cells was based on the frequency of latency within each cell type and the estimated total number of cells.

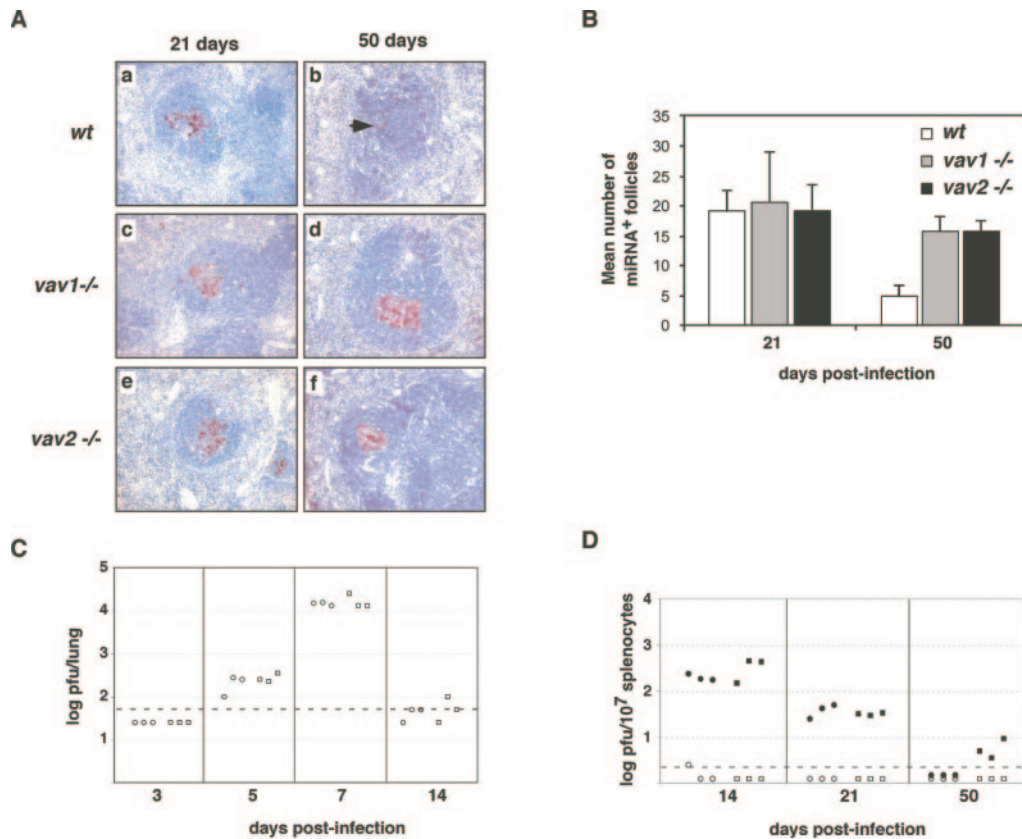


FIG. 6. Persistent MHV-68 infection in *vav1*^{-/-} and *vav2*^{-/-} mice. (A) Wild-type *vav1* or *vav2*-deficient mice were intranasally infected with MHV-68. At the indicated days postinfection, spleens were removed and processed for in situ hybridization using probes derived from miRNAs 1 to 4. Panels show representative spleen sections from each group of animals sampled at 21 (panels a, c, and e) and 50 (panels b, d, and f) days postinfection. All sections are magnified at $\times 200$. (B) Quantification of the mean number of splenic follicles for viral tRNA expression. Error bars represent the standard deviations of the means. Three sections per mouse and at least three mice per group were counted at each time point. (C) Wild-type (circles) and *vav2*-deficient (squares) mice were intranasally infected with 10^4 PFU of MHV-68. Infectious viruses in lungs at the indicated time points after infection were titrated by plaque assay. Each point represents the titer of an individual mouse. The dashed line indicates the limit of detection of the assay. (D) Wild-type (circles) and *vav2*-deficient (squares) mice were intranasally infected with 10^4 PFU of MHV-68. Latent viruses in spleens (closed symbols) were titrated by infectious center assay, whereas preformed infectious viruses (open symbols) were assayed by plaque assay in equivalent freeze-thawed spleen samples. Each point represents the titer of an individual mouse. The dashed line indicates the limit of detection of the assay.

cessation of the expansion of latently infected GC B cells. To approach this issue, we followed the presence of MHV-68 in splenic GCs from animals of the indicated genotypes by in situ hybridization using miRNA riboprobes. The recently identified miRNAs (29) have been shown before to be RNA sequences with tRNA-like sequences located at the 5' end of the MHV-68 genome that are abundantly expressed within GCs of latently infected mice (2, 29, 31, 40). Therefore, they represent excellent markers to monitoring latent viral infections in situ. Wild-type animals showed the expected pattern of miRNA expression upon MHV-68 infection (Fig. 6A). This pattern is characterized by the initial presence of large miRNA-positive clusters of cells within GCs during the establishment of latency (postinfection day 21) and a subsequent decline thereafter (postinfection day 50) (Fig. 6A, panels a and b, and B). As a consequence, the expression of miRNAs became confined to a reduced number of cells scattered within secondary follicles at postinfection day 50 (Fig. 6A, panel b). *vav1*^{-/-} and *vav2*^{-/-} mice showed identical dynamics of miRNA expression relative to wild-type animals during the establishment of la-

tency (Fig. 6A, panels c and e, and B). However, unlike wild-type animals, they still showed large clusters of miRNA-positive cells within GCs at postinfection day 50 (Fig. 6A, panels d and f, and B). The fact that similar results were obtained with *vav1*^{-/-} and *vav2*^{-/-} deficient animals indicates that the full complement of Vav1 and Vav2 proteins is required for optimal M2 function.

We performed two additional experiments to rule out the possibility that the immunodeficiency present in *vav1*^{-/-} and *vav2*^{-/-} mice was responsible for the observed chronic infection of GCs. First, we evaluated the ability of these mice to control primary lytic infection in the lung. Consistent with the absence of clinical signs of infection (data not shown), we observed no differences in the kinetics of virus replication and elimination between *vav2*-deficient mice and C57BL control mice (Fig. 6C). Second, we compared latent infection and lytic infections using ex vivo reactivation assays. No preformed infectious virus could be detected at any of the time points analyzed, indicating that the splenic infection found in *vav2*^{-/-} mice was only latent (Fig. 6D). These results indicate that the

interaction of M2 with Vav proteins is not important for viral infection or the initial establishment of latency. In contrast, it seems to play crucial roles in the termination of the lymphoproliferative amplification of MHV-68 latency in GC B cells.

DISCUSSION

Increasing experimental evidence indicates that the effective colonization of the host by different gammaherpesvirus family members requires the proliferation of latently infected lymphocytes (34). Such a strategy offers an obvious advantage to the virus since proliferating GC B cells facilitate the amplification of viral episomes and, therefore, the subsequent generation of a large reservoir of latent genomes in long-lived memory B cells. In addition, given the restricted level of virus gene expression under these conditions, this strategy also helps viruses to escape from robust immune responses. To make this process effective, gammaherpesviruses have developed molecular mechanisms that promote B-cell stimulation in the absence of cognate antigenic stimulation. Gammaherpesviruses seem to have come out with distinct evolutionary solutions to solve this problem. Thus, EBV and KSHV have developed unique integral transmembrane proteins capable of stimulating B cells by mimicking the normal function of B-cell receptor complexes found at the plasma membrane (9, 20, 21). Instead, MHV-68 lacks genes similar to those described above, suggesting that this virus has developed its own molecular strategies to manipulate the B-cell signaling machinery. In this report, we have shown that one such strategy is the alteration of the signaling pathway regulated by the *vav* family proto-oncogene products via M2, a viral protein previously shown to be necessary for the cessation of the transient expansion of latently infected GC B cells and their differentiation into the memory B-cell pool (32). Thus, MHV-68 appears to have chosen the utilization of a direct downstream element of lymphocyte receptors rather than the receptors themselves for B-cell activation.

A confirmation of the specificity of this interaction is provided by the dramatic effect induced by the expression of M2 on the Vav1 pathway. Thus, we have shown that M2 promotes the activation of the catalytic activity of this exchange factor in the absence of extracellular signals. Such activation is very robust since M2-activated Vav1 can promote levels of Rac1 activation comparable to those observed with highly oncogenic versions of Vav1. The activation of the catalytic activity of Vav1 is due to increased phosphorylation levels of this exchange factor, an event that is mediated by the formation of complexes between Vav1, M2, and Src family members such as Fyn. Interestingly, M2 promotes the phosphorylation of the key Y174 regulatory residue of Vav1 but not of other phosphorylation sites present either in the vicinity (Y¹⁴² and Y¹⁶⁰) or in more distant areas of the Vav1 structure, suggesting that the main goal of the interaction between M2 and Vav1 is the catalytic activation of this GEF. These results are consistent with a scaffold function for M2 that, upon phosphorylation by Fyn, facilitates the assembly of signaling complexes independently of extracellular stimuli or antigens. Interestingly, some viral pathogens unrelated to gammaherpesviruses use similar strategies to favor their fitness in the host cell. The best example is the human immunodeficiency virus, which, upon infec-

tion of T cells, expresses a protein (v-Nef) that binds to Vav1 and activates the Rac1 pathway (12). However, the mechanism of the activation of Vav1 by v-Nef and M2 is totally different since the former molecule does not trigger detectable Vav1 phosphorylation (5). At present, no structural or biochemical information is available regarding the mechanism by which v-Nef stimulates the latent exchange activity of Vav1 in vivo.

The study of the structural determinants involved in the M2/Vav1/Fyn interaction has revealed a high complexity since the optimal binding of both Vav1 and Fyn to M2 requires the dual participation of phosphorylated sequences and a PRR present in this viral protein. The relative dependency of these two binding domains is different between Vav1 and Fyn. Thus, we have observed that the mutation of the M2 PRR totally abolishes the interaction between Vav1 and M2 while it attenuates, but it does not eliminate, the formation of the Fyn/M2 complex. In contrast, we have also seen that the mutation of the M2 phosphorylation sites reduces, but does not abolish, the binding of Vav1 to the viral protein. Instead, the same mutation significantly reduces the association of Fyn with M2. These observations are not consistent with the presence of two independent and insulated binding motifs for Vav1 and Fyn, suggesting instead that cross talk must exist between both regions of M2. Several explanations can be proposed to explain these results. Thus, it is possible that Fyn needs a first contact with the M2 PRR to create a second docking site by favoring the phosphorylation of tyrosines 127 and 136 of M2 and, subsequently, the secondary recruitment of Fyn molecules via the SH2 domain to the phosphorylated sites. Alternatively, it is also plausible that the interaction of the M2 PRR with other potential intracellular targets could be a prerequisite for the colocalization of M2 with Fyn at the plasma membrane that could be potentially required for Fyn binding and M2 phosphorylation. The former possibility is in agreement with our data demonstrating that the M2P2 mutant cannot be fully phosphorylated by Fyn. The requirement of the M2 phosphorylation sites for the optimal binding of Vav1 is less clear since our data indicate that the interaction of the GEF with M2 is totally independent of Fyn overexpression. One possibility is that the stable interaction of Vav1 with M2 would require the simultaneous engagement of its SH3 and SH2 domains via interactions with the PRR and the phosphotyrosine sequences, respectively. The complexity of this interaction also applies to the relative concentrations of each protein within the complex. For example, it is clear that Fyn, although forming a stable complex with M2 and Vav1 when these three proteins are overexpressed, does not have to be in stoichiometric amounts in the M2 complex to induce M2 and Vav1 tyrosine phosphorylation. This fact is exemplified by the observation that M2 (Fig. 5A, lane 1) and Vav1 (Fig. 2A, lane 3, and B) can become phosphorylated in the absence of overexpressed Fyn and, in addition, by the very low levels of association of the endogenous kinase with M2 (Fig. 5A, lane 1) or the M2/Vav1 (Fig. 4D, lane 3) complex as assessed by coimmunoprecipitation experiments and in vitro kinase assays. According to these data, it seems plausible that the action of Fyn on the M2/Vav1 complex is based on a catalytic type of reaction and a rapid "kiss and run" mechanism of association with that complex. In any case, it seems that the phosphorylation reactions in the M2/Vav1 complex are executed exclusively by Src family members

and not by other unrelated kinases since the basal phosphorylation of M2 and Vav1 in the presence or absence of Fyn overexpression is eliminated by specific inhibitors of the enzyme activity of that kinase family.

The physiological relevance of the Vav pathway in M2-mediated viral latency is well illustrated by the persistent high levels of latently infected GC B cells observed in both *vav1*^{-/-} and *vav2*^{-/-} mice upon MHV-68 infection. This phenotype is identical to that recently described by us in the case of M2-deficient MHV-68 recombinants (32), a genetic finding that concurs with the notion that Vav proteins and M2 collaborate in a common signaling pathway. Furthermore, the similar effects observed in the absence of either Vav1 or Vav2 protein suggest that, under normal conditions of infection, M2 requires the simultaneous engagement of both Vav family members to promote its signaling strategy in B cells. Given that both *vav1*- and *vav2*-deficient animals show deficiencies in immune function (37), we performed additional experiments to make sure that the reported observations could not be indirect consequences of the immunodeficiency of those mouse strains. Our results have shown that this potential problem can be ruled out because Vav-deficient mice are fully capable of controlling the acute primary MHV-68 infection in the lung, as assessed by the absence of clinical signs of infection and by the comparable kinetics of viral replication and elimination observed between wild-type and deficient animals. Furthermore, Vav-deficient mice can generate GCs with amplification of virus latency in B cells. Previously published data concur with the above results. Thus, it has been shown that *vav1*^{-/-} mice can mount quite efficient protective cellular and humoral immune responses to other viruses, including vesicular stomatitis and lymphocytic choriomeningitis viruses. Moreover, *vav1*-deficient animals develop GCs with normal morphology in response to vesicular stomatitis virus (1, 28). These results, together with the biochemical and signaling evidence discussed above, confirm the functional connection of M2 and Vav proteins in the regulation of the latency cycle of MHV-68.

The selection of Vav proteins as an intracellular target for M2 offers a distinctive advantage to MHV-68. Vav proteins play essential roles in both T- and B-cell development and during the activation of mature lymphocytes, regulating several Rac1-dependent effects, such as cytoskeletal reorganization or lymphocyte mitogenesis (4, 37). In addition to the activation of Rho/Rac GTPases, Vav proteins also have crucial roles in the indirect activation of other signaling pathways. Thus, it has been shown that the Vav/Rac1 pathway can promote the activation of the Ras route in lymphocytes via the stimulation of RasGRP1, a Ras-specific GDP/GTP exchange factor whose activity is regulated by the second messenger diacylglycerol (6, 42). Similarly, activation of the Rap/integrin pathway via the stimulation of the Rap exchange factor RasGRP2 has also been described previously (7). Vav proteins are also important for the activation of protein kinase C θ and NF-AT (5, 39). Finally, it has been demonstrated that the C-terminal SH3-SH2-SH3 region mediates binding to a wide range of signaling molecules (4, 5). Accordingly, the activation of the Vav/Rac1 pathway by M2 will have a wider impact on cell signaling than the mere activation of its GTPase substrates.

Preliminary evidence indicates that M2 may utilize targets in the cell other than the Vav family. For instance, it is worth

noting the high percentage of putative M2 binding partners with functions related to the cell cytoskeleton observed in our SH3 filter array experiments. These observations suggest that M2 may play a rather multifunctional role in MHV-68 pathogenesis. Further work in this area will give a comprehensive understanding of those pathways that, in turn, will help to shed light into the molecular strategies used by gammaherpesviruses to promote antigen-independent B-cell proliferation and the establishment of life-long latency in the host.

ACKNOWLEDGMENTS

We thank S. Efstathiou for critical reading of the manuscript. We also thank F. Lopes and M. Blázquez for excellent technical help.

This work was supported by grants to J.P.S. from the Portuguese Fundação para a Ciência e Tecnologia (POCTI/ESP/34240/2000) and to X.R.B. from both the U.S. National Cancer Institute (5R01-CA073735-09) and the Spanish Ministry of Education and Science (MES) Biomedicine Program (SAF2003-00028). L.R. and M.M. were recipients of fellowships from the Fundação para a Ciência e Tecnologia. M.J.C. is a researcher of the MES Ramón y Cajal Program.

REFERENCES

- Bachmann, M. F., L. Nitschke, C. Krawczyk, K. Tedford, P. S. Ohashi, K. D. Fischer, and J. M. Penninger. 1999. The guanine-nucleotide exchange factor Vav is a crucial regulator of B cell receptor activation and B cell responses to nonreplicative antigens. *J. Immunol.* **163**:137–142.
- Bowden, R. J., J. P. Simas, A. J. Davis, and S. Efstathiou. 1997. Murine gammaherpesvirus 68 encodes tRNA-like sequences which are expressed during latency. *J. Gen. Virol.* **78**:1675–1687.
- Bustelo, X. R. 2002. Regulation of Vav proteins by intramolecular events. *Front. Biosci.* **7**:d24–d30.
- Bustelo, X. R. 2000. Regulatory and signaling properties of the Vav family. *Mol. Cell. Biol.* **20**:1461–1477.
- Bustelo, X. R. 2001. Vav proteins, adaptors and cell signaling. *Oncogene* **20**:6372–6381.
- Caloca, M. J., J. L. Zugaza, D. Matallanas, P. Crespo, and X. R. Bustelo. 2003. Vav mediates Ras stimulation by direct activation of the GDP/GTP exchange factor Ras GRP1. *EMBO J.* **22**:3326–3336.
- Caloca, M. J., J. L. Zugaza, M. Vicente-Manzanares, F. Sanchez-Madrid, and X. R. Bustelo. 2004. F-actin-dependent translocation of the Rap1 GDP/GTP exchange factor RasGRP2. *J. Biol. Chem.* **279**:20435–20446.
- Crespo, P., K. E. Schuebel, A. A. Ostrom, J. S. Gutkind, and X. R. Bustelo. 1997. Phosphotyrosine-dependent activation of Rac-1 GDP/GTP exchange by the *vav* proto-oncogene product. *Nature* **385**:169–172.
- Damania, B. 2004. Oncogenic gamma-herpesviruses: comparison of viral proteins involved in tumorigenesis. *Nat. Rev. Microbiol.* **2**:656–668.
- Davison, A. J. 2002. Evolution of the herpesviruses. *Vet. Microbiol.* **86**:69–88.
- Etienne-Manneville, S., and A. Hall. 2002. Rho GTPases in cell biology. *Nature* **420**:629–635.
- Fackler, O. T., W. Luo, M. Geyer, A. S. Alberts, and B. M. Peterlin. 1999. Activation of Vav by Nef induces cytoskeletal rearrangements and downstream effector functions. *Mol. Cell* **3**:729–739.
- Flano, E., I. J. Kim, J. Moore, D. L. Woodland, and M. A. Blackman. 2003. Differential gamma-herpesvirus distribution in distinct anatomical locations and cell subsets during persistent infection in mice. *J. Immunol.* **170**:3828–3834.
- Flano, E., I. J. Kim, D. L. Woodland, and M. A. Blackman. 2002. Gamma-herpesvirus latency is preferentially maintained in splenic germinal center and memory B cells. *J. Exp. Med.* **196**:1363–1372.
- Ganem, D. 1997. KSHV and Kaposi's sarcoma: the end of the beginning? *Cell* **91**:157–160.
- Herskowitz, J., M. A. Jacoby, and S. H. Speck. 2005. The murine gamma-herpesvirus 68 M2 gene is required for efficient reactivation from latently infected B cells. *J. Virol.* **79**:2261–2273.
- Husain, S. M., E. J. Usherwood, H. Dyson, C. Coleclough, M. A. Coppola, D. L. Woodland, M. A. Blackman, J. P. Stewart, and J. T. Sample. 1999. Murine gammaherpesvirus M2 gene is latency-associated and its protein a target for CD8⁺ T lymphocytes. *Proc. Natl. Acad. Sci. USA* **96**:7508–7513.
- Jacoby, M. A., H. W. Virgin IV, and S. H. Speck. 2002. Disruption of the M2 gene of murine gammaherpesvirus 68 alters splenic latency following intranasal, but not intraperitoneal, inoculation. *J. Virol.* **76**:1790–1801.
- Jensen, K. K., S. C. Chen, R. W. Hipkin, M. T. Wiekowski, M. A. Schwarz, C. C. Chou, J. P. Simas, A. Alami, and S. A. Lira. 2003. Disruption of CCL21-induced chemotaxis in vitro and in vivo by M3, a chemokine-binding protein encoded by murine gammaherpesvirus 68. *J. Virol.* **77**:624–630.
- Lagunoff, M., R. Majeti, A. Weiss, and D. Ganem. 1999. Deregulated signal

- transduction by the K1 gene product of Kaposi's sarcoma-associated herpesvirus. *Proc. Natl. Acad. Sci. USA* **96**:5704–5709.
21. Lee, H., J. Guo, M. Li, J. K. Choi, M. DeMaria, M. Rosenzweig, and J. U. Jung. 1998. Identification of an immunoreceptor tyrosine-based activation motif of K1 transforming protein of Kaposi's sarcoma-associated herpesvirus. *Mol. Cell. Biol.* **18**:5219–5228.
 22. Liang, X., Y. C. Shin, R. E. Means, and J. U. Jung. 2004. Inhibition of interferon-mediated antiviral activity by murine gammaherpesvirus 68 latency-associated M2 protein. *J. Virol.* **78**:12416–12427.
 23. Lopez-Lago, M., H. Lee, C. Cruz, N. Movilla, and X. R. Bustelo. 2000. Tyrosine phosphorylation mediates both activation and downmodulation of the biological activity of Vav. *Mol. Cell. Biol.* **20**:1678–1691.
 24. Macrae, A. I., E. J. Usherwood, S. M. Husain, E. Flano, I. J. Kim, D. L. Woodland, A. A. Nash, M. A. Blackman, J. T. Sample, and J. P. Stewart. 2003. Murid herpesvirus 4 strain 68 M2 protein is a B-cell-associated antigen important for latency but not lymphocytosis. *J. Virol.* **77**:9700–9709.
 25. Madureira, P. A., P. Matos, I. Socio, L. K. Dixon, J. P. Simas, and E. W. Lam. 2005. Murine gamma-herpesvirus 68 latency protein M2 binds to Vav signaling proteins and inhibits B-cell receptor-induced cell cycle arrest and apoptosis in WEHI-231 B cells. *J. Biol. Chem.* **280**:37310–37318.
 26. Marques, S., S. Efstathiou, K. G. Smith, M. Haury, and J. P. Simas. 2003. Selective gene expression of latent murine gammaherpesvirus 68 in B lymphocytes. *J. Virol.* **77**:7308–7318.
 27. McGeoch, D. J., D. Gatherer, and A. Dolan. 2005. On phylogenetic relationships among major lineages of the Gammaherpesvirinae. *J. Gen. Virol.* **86**:307–316.
 28. Penninger, J. M., K. D. Fischer, T. Sasaki, I. Kozieradzki, J. Le, K. Tedford, K. Bachmaier, P. S. Ohashi, and M. F. Bachmann. 1999. The oncogene product Vav is a crucial regulator of primary cytotoxic T cell responses but has no apparent role in CD28-mediated co-stimulation. *Eur. J. Immunol.* **29**:1709–1718.
 29. Pfeffer, S., A. Sewer, M. Lagos-Quintana, R. Sheridan, C. Sander, F. A. Grasser, L. F. van Dyk, C. K. Ho, S. Shuman, M. Chien, J. J. Russo, J. Ju, G. Randall, B. D. Lindenbach, C. M. Rice, V. Simon, D. D. Ho, M. Zavolan, and T. Tuschl. 2005. Identification of microRNAs of the herpesvirus family. *Nat. Methods* **2**:269–276.
 30. Schuebel, K. E., N. Movilla, J. L. Rosa, and X. R. Bustelo. 1998. Phosphorylation-dependent and constitutive activation of Rho proteins by wild-type and oncogenic Vav-2. *EMBO J.* **17**:6608–6621.
 31. Simas, J. P., and S. Efstathiou. 1998. Murine gammaherpesvirus 68: a model for the study of gammaherpesvirus pathogenesis. *Trends Microbiol.* **6**:276–282.
 32. Simas, J. P., S. Marques, A. Bridgeman, S. Efstathiou, and H. Adler. 2004. The M2 gene product of murine gammaherpesvirus 68 is required for efficient colonization of splenic follicles but is not necessary for expansion of latently infected germinal centre B cells. *J. Gen. Virol.* **85**:2789–2797.
 33. Simas, J. P., D. Swann, R. Bowden, and S. Efstathiou. 1999. Analysis of murine gammaherpesvirus-68 transcription during lytic and latent infection. *J. Gen. Virol.* **80**:75–82.
 34. Stevenson, P. G. 2004. Immune evasion by gamma-herpesviruses. *Curr. Opin. Immunol.* **16**:456–462.
 35. Stevenson, P. G., S. Efstathiou, P. C. Doherty, and P. J. Lehner. 2000. Inhibition of MHC class I-restricted antigen presentation by gamma 2-herpesviruses. *Proc. Natl. Acad. Sci. USA* **97**:8455–8460.
 36. Thorley-Lawson, D. A. 2001. Epstein-Barr virus: exploiting the immune system. *Nat. Rev. Immunol.* **1**:75–82.
 37. Turner, M., and D. D. Billadeau. 2002. VAV proteins as signal integrators for multi-subunit immune-recognition receptors. *Nat. Rev. Immunol.* **2**:476–486.
 38. Usherwood, E. J., J. P. Stewart, and A. A. Nash. 1996. Characterization of tumor cell lines derived from murine gammaherpesvirus-68-infected mice. *J. Virol.* **70**:6516–6518.
 39. Villalba, M., K. Bi, J. Hu, Y. Altman, P. Bushway, E. Reits, J. Neeffjes, G. Baier, R. T. Abraham, and A. Altman. 2002. Translocation of PKC[theta] in T cells is mediated by a nonconventional, PI3-K- and Vav-dependent pathway, but does not absolutely require phospholipase C. *J. Cell Biol.* **157**:253–263.
 40. Virgin, H. W., IV, P. Latreille, P. Wamsley, K. Hallsworth, K. E. Weck, A. J. Dal Canto, and S. H. Speck. 1997. Complete sequence and genomic analysis of murine gammaherpesvirus 68. *J. Virol.* **71**:5894–5904.
 41. Willer, D. O., and S. H. Speck. 2003. Long-term latent murine gammaherpesvirus 68 infection is preferentially found within the surface immunoglobulin D-negative subset of splenic B cells in vivo. *J. Virol.* **77**:8310–8321.
 42. Zugaza, J. L., M. J. Caloca, and X. R. Bustelo. 2004. Inverted signaling hierarchy between RAS and RAC in T-lymphocytes. *Oncogene* **23**:5823–5833.